Electrode Architecture

International Edition: DOI: 10.1002/anie.201507780
German Edition: DOI: 10.1002/ange.201507780

Electrode Architecture in Galvanic and Electrolytic Energy Cells

Beomgyun Jeong[+], *Joey D. Ocon*[+], *and Jaeyoung Lee**

batteries · electrode construction · fuel cells · water oxidation

Electrodes in galvanic and electrolytic energy cells are complicated structures comprising redox-active materials, ionic/electronic conductors, and porous pathways for mass transfer of reactants. In contrast to breakthroughs in component development, methods of optimizing whole-system architectural design to draw maximum output have not been well explored. In this Minireview, we introduce generalized types of electrode architecture, discuss fabrication strategies, and characterize already built structures. Systematic efforts to discover optimal electrode configurations will resolve long-standing discrepancies that arise between whole systems and the sums of their parts for a number of electrochemical reactions and technologies.

1. Introduction

The term "electrode" was first coined from the Greek words *elektron* (from which electricity is derived) and *hodos* (a way). The following four processes occur at electrode/electrolyte interfaces in series:[1]

1) chemical reactants approach the electrode surface,
2) the reactants adsorb onto the electrode surface,
3) charge is transferred between the reactants and the electrode,
4) the resulting product desorbs and leaves the electrode surface.

In half-cell reactions of galvanic and electrolytic cells, the charge transfer rate between the electrode and the reactant dictates the overall rate of the electrochemical process, which is why electrocatalysis is considered an important theme in electrochemistry.[2] However, the rate of electron transfer through the electrode/electrolyte interface, the ionic/electronic conductivity, and the rate of reactant/product transport also govern the overall reaction rate. Therefore, achieving a balance between electron/ion conducting media volumes for redox reactions and open pore space for mass transport is essential;[3] this can be accomplished by carefully designing electrode structures.

To achieve balance between component phases, the area or length of the interphase, where the electrocatalyst or electroactive material, electrolyte, current collector, and chemical-reactant pathway meet, should be considered. Because noble metals are extremely expensive, finely dispersed nanoparticles attached to conducting supports (e.g., porous carbon and conductive metal oxides) are used as electrocatalysts to increase surface-volume ratio and/or surface-mass ratio.[4,5] This approach enables a reduction of the total cost, and also improves the power density of galvanic cells and the energy efficiency of electrolytic cells. In addition to increasing the surface area of an electrode, the interphase connection from the electrode surface to the ion/electron conducting media must be established, as well as the availability of open pore spaces for reactant/product. For example, the use of Pt nanoparticles supported on highly porous and electron-conducting carbon black (Pt/C) is a significant breakthrough in fuel-cell technology in terms of providing a much larger Pt surface area; however, more than half of the area provided by the Pt nanoparticles is not utilized for fuel-cell reactions[6] owing to incomplete connections between Pt sites and the ion-conducting medium network.[7] Hence, architecturally designing electrode surfaces for better utilization efficiency has far-reaching implications for "green" energy-storage and conversion technologies, such as capacitors, batteries, fuel cells, and electrolyzers.

---

[*] Dr. B. Jeong,[+] Prof. J. D. Ocon,[+] Prof. Dr. J. Lee
School of Environmental Science and Engineering
Ertl Center for Electrochemistry and Catalysis
Gwangju Institute of Science and Technology (GIST)
Gwangju 61005 (South Korea)
E-mail: jaeyoung@gist.ac.kr

Prof. J. D. Ocon[+]
Laboratory of Electrochemical Engineering (LEE) Department of Chemical Engineering, University of the Philippines Diliman
Quezon City (Philippines)

[+] These authors contributed equally to this work.

Stability is another aspect that should be considered in electrode fabrication. Presently, the use of Si-based anodes in lithium-ion batteries is a popular alternative to commercial graphite anodes owing to their high energy capacity, but their dimensional instability creates a formidable technological barrier.[8] The development of a structure-preserving interface even in cases of electrode-dimension change could alleviate this problem. Chemical oxidation of electrodes could be prevented by introducing a protective component layer or a dimensionally stable support.[5] However, introducing new catalyst-support materials may lead to a combination of adverse effects, such as decreases in activity, mass transport, and conductivity. Therefore, to minimize these adverse effects, any new material that is introduced into an electrochemical system must first be tuned with respect to the electrode structure. In addition, establishing a uniform reaction-rate distribution over the interphase is an important objective in electrode design to minimize over- or under-utilized sites and provide better stability and performance of the overall system.[9]

Considering that the objective of an electrode's structure is the efficient and sustainable utilization of electrode components and space, electrode development could be viewed as analogous to architecture, which is defined as both the process and product of planning, designing, and constructing buildings and other physical structures (Figure 1). The analogous relationship between architecture and electrode development has been well described in several reviews on battery applications and heterogeneous catalysis.[10–12] For instance, one such review focused on the use of 3D nanoarchitectures for lithium-battery applications and discussed the effects of pore space (void) and periodicity in electrode design for fuel-cell applications.[3]

Herein, we provide a focused review of the generalized architectural types that can be found in various electrode systems used for chemical energy conversion and storage and discuss the pros and cons of these architectural types in terms of electron/ion conduction, mass transfer of molecular reactant/product, extent of the interphase network, and structural stability. We also introduce synthesis techniques and provide representative examples of different forms of electrode architecture. Recent advances in microscopy and tomography techniques for the examination of 3D structures and the use of operando analysis to probe electrode/electrolyte interfaces are also discussed, as these methods are fundamentally important toward understanding the architectural design of electrodes. Finally, we provide a perspective on the ideal electrode architecture based on the concept of inducing process homogeneity from structural heterogeneity and discuss how the ideal electrode architecture can be substantiated using advanced electrochemical crystallization and self-assembling synthesis techniques.

2. Electrode Architecture for Electrochemistry

The architecture of an electrochemical cell is based on electrochemically active materials, electrically conductive agents, and electrolytes as building blocks. Although the improvement of the material properties of these building blocks is important, research into their ideal configuration within an electrode has received more attention because electrodes are highly complex systems with many interfaces, which can be described well by the adage "The whole is more than the sum of its parts.".

The major criteria that need to be considered in electrode structural design include the transport resistance in the networks of various phases, the areas or lengths of interphases, and structural stability. In cases where expensive materials must be used in an electrode, the utilization efficiency and the effectiveness factor are additional important criteria of electrode architecture that must be considered for economic feasibility. Electrochemical processes occur at the interface of multiple phases in an electrode, thus the most crucial objective of electrode architecture is maximizing the number of networked interfacial sites.

We introduce the case of a fuel-cell electrode as an example of a system that places immense importance on electrode structure, as fuel-cell electrodes utilize a three-phase boundary (TPB), which is composed of gas, ion, and

Beomgyun Jeong is a post-doc scientist working at the Ertl Center for Electrochemistry and Catalysis, Gwangju Institute of Science and Technology (GIST) and a visiting scientist at the Advanced Light Source in Lawrence Berkeley National Laboratory. He took his PhD under Prof. Dr. Jaeyoung Lee in GIST, South Korea on oxygen electrodes in alkaline fuel cell and water electrolysis based on transition-metal-modified carbon nanofibers. His current research interest is operando ambient pressure XPS analyses for electrocatalyst degradation and electrode corrosion phenomena.

Joey D. Ocon is an assistant professor of Chemical Engineering at the University of the Philippines Diliman, where he obtained his BSc and MSc degrees in Chemical Engineering in 2008 and 2011, respectively. In 2015, he received his PhD degree from GIST (South Korea) on the development of semiconductor-air alkaline batteries in Prof. Jaeyoung Lee's group. His research interests include rechargeable Zn-air batteries, oxygen electrocatalysis in fuel cells and metal-air batteries, and CO_2 reduction.

Jaeyoung Lee is the vice director of the Ertl Center for Electrochemistry and Catalysis and a full professor at the School of Environmental Science and Engineering at GIST, South Korea. He took his PhD with Prof. Gerhard Ertl's (2001) from the Fritz-Haber-Institut der Max-Planck-Gesellschaft and FU Berlin, Germany. He was a senior scientist at the RIST/POSCO (2002–2004) and at the Fuel Cell Research Center, KIST (2004–2007). His current research interests include oxygen electrocatalysis, fuels from CO_2, and operando spectroscopic analyses for electrochemical systems.

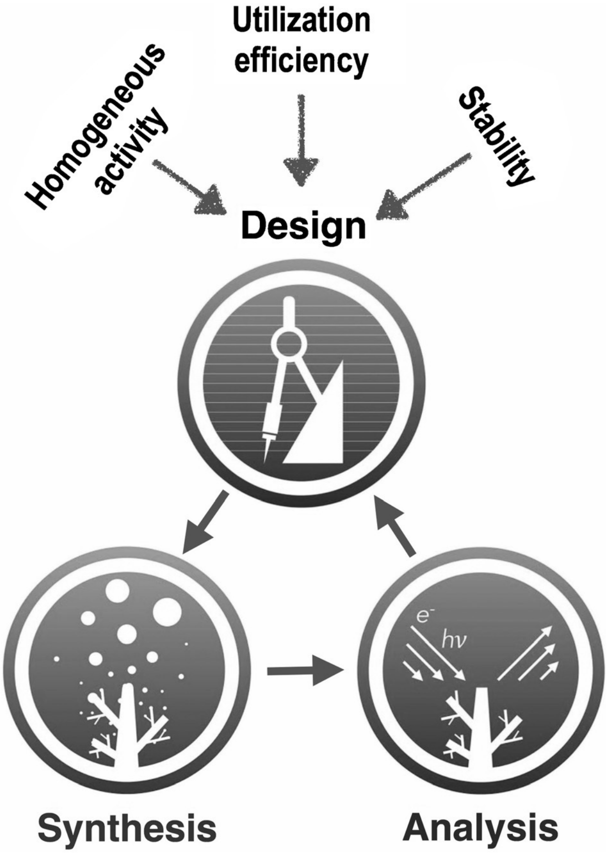

Figure 1. Conceptual electrode-fabrication strategy to optimize the utilization efficiency, activity, and stability of electrodes. The strategy uses an architectural blueprint derived from multi-scale modeling of ideal backbone structures for electrode fabrication and characterization, and provides feedback during the design stage. This conceptual strategic procedure is now achievable through the development of multi-scale fabrication techniques and analytical methods based on electron, X-ray, and 3D imaging and interface-probing technologies.

electron phases. In comparing the geometrical surface areas of particles and the electrochemical surface area (ECSA), it can be identified that approximately 50 % of the Pt present is not participating in electrochemical processes.[4,13] Moreover, according to multi-scale simulations conducted for polymer electrolyte membrane fuel cells (PEMFC) electrodes, approximately 90 % of a catalyst surface that has been prepared by conventional methodology does not participate in the oxygen reduction reaction (ORR) because there is an insufficient number of interfacial contacts between the catalytic sites, the void space, and the conductive agents for mass and electronic transfer.[14] A reasonably designed and constructed three-phase boundary structure further reduces the use of expensive noble metal catalysts and thus widens the window of opportunity for the use of non-noble metal-based electrocatalysts.

Various structures have been suggested in many studies for achieving this purpose; they can be categorized into two general architectural types: interconnected fractal structures and ordered array structures. Below, we discuss the advantages and disadvantages of each architectural type and introduce the related studies.

2.1. Interconnected Fractal Structures

In general, the pore structure of an electrode is typically formed by the aggregation of porous carbon particles to give mass fractal patterns (Figure 2 a).[15] The main strengths of the fractal structure are its large accessible surface area of electrocatalytic or electroactive material and minimal transfer resistance when structural parameters are optimized (e.g., thickness, number of hierarchy level, pore size scale of lowest level, size distribution, and volume ratio between different phases).[15] These geometrical parameters are determined according to mass and ionic transport and electrical conductivity. As a result of the discoveries of various nano-sized carbon allotropes (especially CNT and graphene), various types of electrically conductive networks are now available.[16,17]

In the case of electrochemical capacitors, two phases within a 3D volume meet to form a 2D interphase surface. The ideal electrode for an electrochemical capacitor would have a fractal pore structure. Such a structure provides the largest area of available electrode/electrolyte interface and also facilitates unhindered ionic conduction through the electrolyte-filled pore network. Conventional electrochemical capacitors also have hierarchical pore structures, with macro-pores being formed by the agglomeration of carbon black particles and the meso- and micropores reside inside each carbon black particle (Figure 2 b).[18]

On the other hand, in batteries and fuel cells, three phases are involved in forming interfaces. For example, in PEMFC, there are three phases, including Pt, void space, and Nafion, and two interphase surfaces, including Pt/void and Pt/Nafion. They form a three-phase boundary consisting of Pt, void, and Nafion with a closed 1D loop form.[21,22] One ideal architectural type that can be imagined for fuel-cell electrodes is the use of hierarchically porous and electronically conductive medium on the gas reactant side and the inclusion of a very thin catalyst particle layer on the surface of the ionic conducting media, such that every catalyst particle forms a connection to the ionic/electronic conducting media network and also to the void network for reactant transfer (Figure 2 c,d).[19] The currently employed synthesis technique is based on random mixing of electrode components while expecting serendipitous formation of interphase connections within the electrode structure. However, this synthesis approach is not enough for the complete and reliable interphase formation, as exemplified by the low utilization efficiency and effectiveness factor of Pt in fuel-cell electrodes. Bottom-up and self-assembling synthesis techniques for the complete formation of the interphase is necessary for resolving this issue, which we will describe in Section 3.

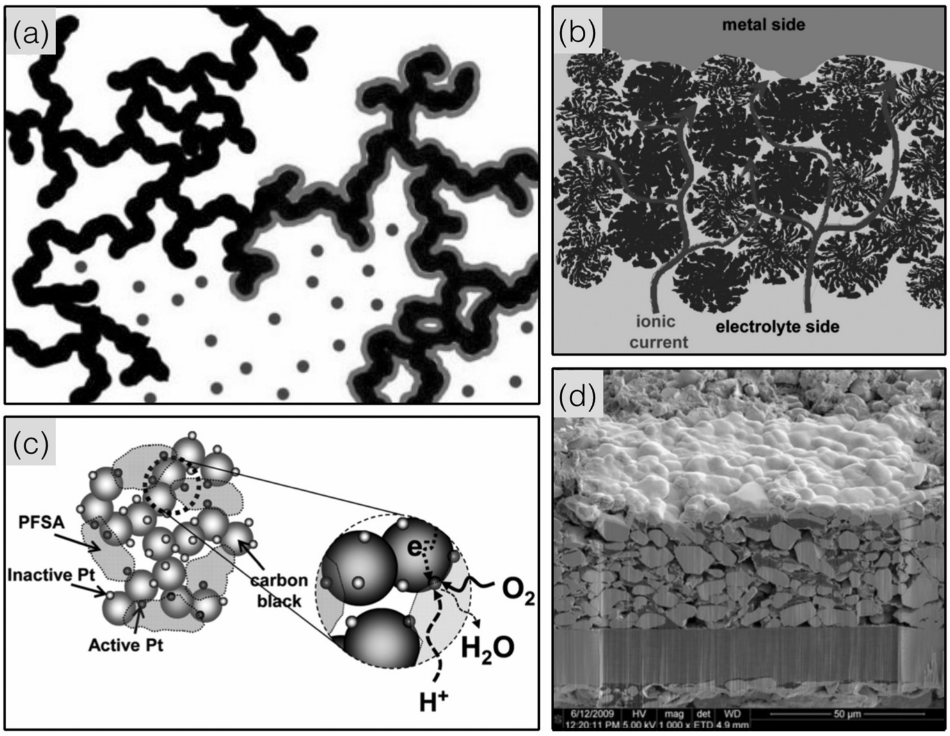

Figure 2. a) Mass fractal surface structure formed by the aggregation of small particles (http://www.fractal.org/Life-Science-Technology/Publications/Pore-fractal.htm); b) Electrode structure in an electrical double-layer capacitor, typically formed by carbon-black particles;[18] c) three-phase boundary structure in a hydrogen fuel-cell electrode;[19] d) Porous structure of a cathode layer in a lithium-ion battery.[20]

2.2. Ordered Array Structures

Another general architectural type for electrodes is the use of a small or thin (ca. 1 μm) ordered array of 1D rods or 2D platelets. Compared with fractal structures, this configuration provides a lower area of catalytically active sites, but it offers the following advantages:

- Larger statistical fraction of electrocatalyst near the three-phase boundary
- Lower transport resistance at the three-phase boundary
- Well-defined and controllable fabrication
- Continuous production is possible
- Larger catalyst unit could be more stable

Developments in template preparation methodology have enabled the creation of various forms of ordered-array-type electrodes. Nanostructured thin film (NSTF) electrodes have been developed for Pt-catalyst-based fuel cells.[23] These are comprised a thin layer, with a thickness of approximately 0.25 μm, which contains vertically aligned whiskers approximately 50 nm in diameter coated with Pt (Figure 3 a,b). Larger grain sizes can be deposited on the whisker structures, leading to lower surface area (10–25 m^2g^{-1}) compared to Pt/C-based electrodes (30–45 m^2g^{-1}); however, 5- to 10-fold greater specific activity is attained, resulting in greater exchange current density and better resistance to dissolution. Thinner electrode layers have shorter transfer paths, allowing lower transfer resistance and increasing the chances for catalytic sites to become connected to the ionic phase, eventually increasing the statistical fraction of electrocatalyst at the three-phase boundaries. In this architectural type, the carbon support is excluded, and the Pt layer serves as the electrically conductive medium. This configuration reduces the carbon/carbon contact resistance of Pt/C agglomeration and also eliminates carbon corrosion, thereby improving chemical stability.[14,23,24]

Ordered mesoporous carbons into which Fe and N are doped, show promising ORR performance in oxygen-containing acid and alkaline solutions. In this electrocatalyst architecture, catalytic sites are distributed on a large area of mesopores, increasing the accessibility of electrolytes and gaseous reactants to the active sites (Figure 3 c,d). These catalysts show very promising half-cell performance in terms of comparable activity and stability to Pt/C catalysts. In a single cell test, however, the power density performance is lower than expected in a half-cell test. This discrepancy suggests the necessity of developing a new optimized electrode structure and fabrication technique that reduces Ohmic and concentration losses.

2.3. Electrode Stability

Electrode instability originates not only from chemical changes in the electroactive materials but also from structural collapse resulting from the dimensional change in an electrode. ORR electrocatalysts for fuel cells, such as Pt/C and Fe-N_x-C, have the issue of carbon corrosion at highly anodic potentials, causing a loss of Pt nanoparticles or Fe-N_x active sites from graphitic carbon supports.[28,29] To solve the

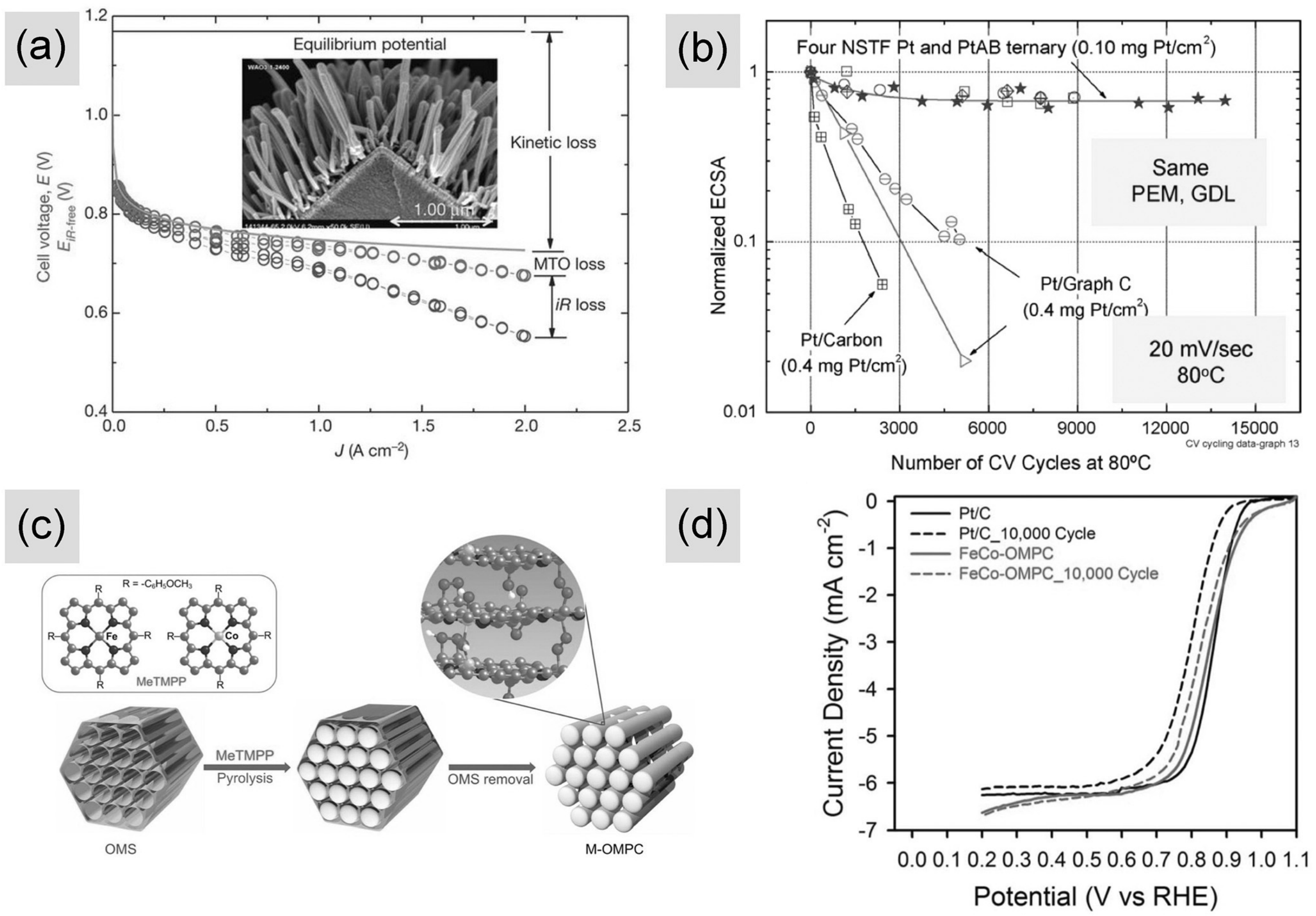

Figure 3. a) Nanostructured thin film (NSTF) electrode with whisker array structure for use in hydrogen fuel cells and its performance represented with an *I–V* curve;[25] b) Stability testing results for NSTF electrodes and of Pt/C and Pt/graphitic carbon catalysts; PEM = polymer electrolyte membrane and GDL = Gas diffusion layer,[26] c) Ordered mesoporous pyrolytic carbon (OMPC) for oxygen reduction reaction with a rod array structure;[27] d) Electrocatalytic activity of OMPC and of Pt/C in acid media.[27]

limitations imposed by the use of carbon supports in fuel cells, electrically conductive TiO_2 nanoparticles have been considered as alternative support materials.[5] Although TiO_2 is dimensionally stable, it loses electrical conductivity at highly anodic potentials, resulting in increased cell resistance. To replace carbon with TiO_2 as an electrocatalyst support, a different type of architecture in which Pt particles participate in the electrically conductive network in addition to TiO_2 particles would be necessary. In addition, TiO_2 is more hydrophilic than carbon when used in electrodes, so a different mode of water management must be considered in this architectural design.

In batteries, minimizing the stress caused by electrode dimension changes during charge–discharge cycling is a major technical problem in terms of improving the recyclability of lithium batteries with non-graphitic anodes. Recently, the use of Si-based anodes in Li-ion batteries has been studied because of their very high specific capacity relative to graphitic anodes. However, volume expansion during Li alloying causes dimensional instability in the cell and subsequent interfacial breakage. Improving electrode architecture could provide ways to relieve the stress caused by volume change and also minimize interface collapse. Electrodes composed of ordered arrays of Si rods allow some space for volume expansion, providing a conductive path to the current collectors.[8,30] A hierarchical porous structure can also be used with this type of electrode material to accommodate volume expansion.[31]

Aside from dimensional instability, the performance robustness of electrode architecture in various environments is also important. For example, NSTF electrodes shows excellent performance under optimized conditions and improved chemical stability resulting from the absence of a carbon support in the electrode architecture, however, the performance of the NSTF is susceptible to the environment and operation condition (e.g., start-up, flooding situations, and operation at non-ideal temperatures) due to its low electrochemical surface area and thin catalyst layer.[32,33] To mitigate this concern, a well-designed balance of plant (BOP) or additional local architecture for regulating the local environment near electrocatalysts should be pursued in future studies.

A homogeneous distribution of reaction rates is important for the utilization efficiency of electrochemically active interfaces and also for the stability of the electrode performance, because over-used active sites become unstable faster and the overall electrode performance would be lowered accordingly. To make the reaction rate over the electrode surface uniform, it was attempted to distribute the catalysts heterogeneously with a 2D pattern on the electrode.[9,34] Fundamental studies on the spatiotemporal pattern of the electrochemical reaction rate on the electrode were performed,[35–37] and deeper understanding via a further study of these phenomena might help in designing more stable electrode architectures with spatially and temporally uniform electrochemical reaction rates over the electrode surface.

3. Synthesis Approaches

As discussed in the preceding Sections, different synthesis techniques have been used to fabricate various electrode architectures. Generally, ideally combined hierarchical porous materials provide good electrode structures for electrochemical applications.[38–40] A wide array of synthetic approaches has been proposed for the creation of these ideal nanostructures, which can be grouped into either top-down or bottom-up approaches (Figure 4). In the top-down approach, electrodes are synthesized by successively slicing or cutting bulk material. This includes using soft and hard templates, high-precision machinery, size reduction, or main-component dissolution.[41–43]

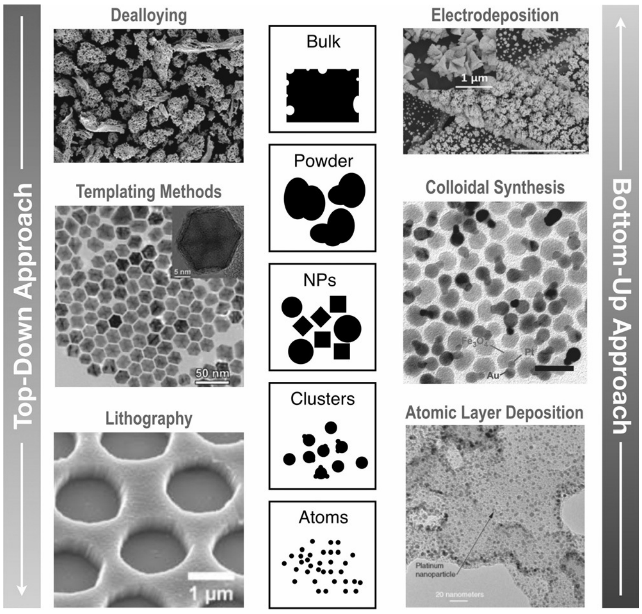

Figure 4. Two major contrasting but complementary approaches in the synthesis or fabrication of electrodes for energy conversion applications: the top-down approach (left) and the bottom-up approach (right).

In the bottom-up approach, the electrode is built up atom-by-atom, molecule-by-molecule, cluster-by-cluster, and particle-by-particle. For example, electrodes have been fabricated using underpotential electrodeposition (UPD), layer-by-layer deposition (LBL), colloidal synthesis, atomic layer deposition (ALD), and molecular layer deposition (MLD) for conformal coating of thin layers on a substrate.[44,45]

The choice of the method depends on architectural scale. The bottom-up approach is the preferred choice for building up the nanoscale structure. The essence of the electrode architecture formation from vapor, liquid, or solid phase in the bottom-up approach is the nucleation and growth. As the concentrations of the building blocks (atoms, ions, or molecules) of a solid increase up to a critical point, aggregates of small clusters (nuclei) form via homogeneous nucleation. Providing a continuous supply of the building blocks enables the nuclei to serve as seeds for further growth of larger structures. Vapor-phase synthesis has been an extensively explored technique for the formation of 1D nanostructures, such as whiskers, rods, and wires,[46] which are crucial components in ordered-array electrode architectures from a variety of materials.[47–52] Not only atomic assembly, nanoparticle self-assembly via sintering and chain connection is another bottom-up approach used to fabricate larger aspect ratio structures of different elements in compounds on various scales.[53–55]

The top-down approach is the better choice for making meso- and macro-scale structures. Inhomogeneity in interconnected fractal structures allows homogeneous mass and charge transfer in a larger scale electrode structure. For mass or charge transfer, there should be a lower limit of scale for the void-network and building-block components,[56] then on that small scale level, each electrode component, including pore space, would have the same size and does not have to be distributed in a fractal configuration. Thus, it would be wise to combine these pathways according to the scale of architecture; preparation of macro- to meso-scale architectures via the top-down approach whereas the bottom-up approach is better suited for the modification of the surface inside a larger structure by using nano-scale catalysts and electroactive materials to introduce desirable functionalities. As emphasized by Rolison et al. in 3D battery electrode architectures, as pore size decreases to less than 100 nm, the nature of the void volume becomes crucial to facilitate solvent infiltration, ion transport, and mass transport.[12] Thus, the surface of the void volume should be completely and uniformly modified with electroactive materials. Various methodologies exist for the deposition of such self-limiting thin films on electrodes, such as ALD.[57]

However, a large gap exists between actually fabricated electrodes and ideal electrode structure in terms of the reliability and completeness of the interphase connection. In the case of solid-electrolyte-based electrochemical cells, electrode/electrolyte interfaces are formed with a certain statistical probability when the electrode layer is attached onto the membrane by direct coating or a decal transfer technique. The probability that the catalyst is located near the three-phase boundary dramatically drops with increasing layer thickness, leading to a loss of catalyst utilization efficiency despite the large surface area provided by the thicker layer. In batteries and capacitors, electrochemically active agents are randomly mixed with binders and electrically conductive graphite powders, and the mixture is attached onto current-collecting foil as shown in Figure 2d.[20]

In this structure, misconnections can exist among the present species. To attain an ideal electrode architecture that achieves the full extent of a catalyst's or active material's utilization efficiency, a bottom-up process that can form catalytic sites spontaneously and selectivity at electrolyte/void interfaces and also forms contacts with a current-collection network is desired.

In this context, electrodeposition techniques provide a way to create such structures of catalytic electrodes and particles, selectively interconnected to void and electrolyte phases.[59,60] Electrodeposition is an old technique for coating a metal layer onto a conductive substrate by applying an electrochemical potential. It is a bottom up synthesis approach that can be used for catalyst preparation.[24,61] Since metal-ion reduction only occurs at electrochemically active surfaces, the electrodeposition technique allows the formation of catalysts or electroactive materials selectively at the interphase sites where electrical and ionic phases are connected. For example, electrochemical deposition has been proposed as way of achieving the selective formation of catalysts at the three-phase boundary (Figure 5).[58,62] A gas-diffusing electrode is immersed in an aqueous solution of Pt salt and Nafion ionomer, and an electrical potential is applied in pulses to electrochemically reduce the Pt ions into small Pt nanoparticles, which together with Nafion aggregates (ion-conducting branches) are deposited on the hydrophilic carbon support. As a result of the minimization of unutilized Pt surface through the selective formation of Pt at the ionically and electrically connected interphase, this method could reduce the required loading amount of a catalyst to a sixth of its present value and produce slightly higher power density than conventionally prepared Pt/C electrodes. In addition to building up electrocatalysts that are selectively interconnected to ionic and electronic media, deeper understanding on this technique would be useful for studying the structural effects of Li active materials in Li-ion or Li-air batteries to deal with battery failure caused by Li dendrite formation.

Another interesting bottom-up approach for building up nanoscopic uniform structures is the use of metal–organic frameworks (MOF). These are ordered networks of a metallic center units and organic linkers, resulting in a well-defined nano-size pore matrix with very large specific surface area and pore volume.[63] The potential of this material for electrode architecture relies on the vast diversity in the size and chemical environment of the crystal pores, which can be tailored for a given application by adjusting the metallic centers and organic linkers.[64] Owing to the large surface area and pore volume, MOFs could be used for electrolytic and galvanic cells that require large surface areas with well-defined and controlled architectures. Since MOFs are usually electrical insulators, direct application of MOFs is limited to batteries in which the low conductivity of the electroactive material can be overcome by mixing small electroactive MOF particles with conductive carbon, as shown in the case of insulating $LiFePO_4$ particles in Li-ion batteries.[65,66] Instead of using a MOF as it is, it can be used as a template to prepare highly ordered microporous carbon by the carbonization of the MOF for electric double-layer capacitors or pyrolyzed N-doped carbon for ORR.[67]

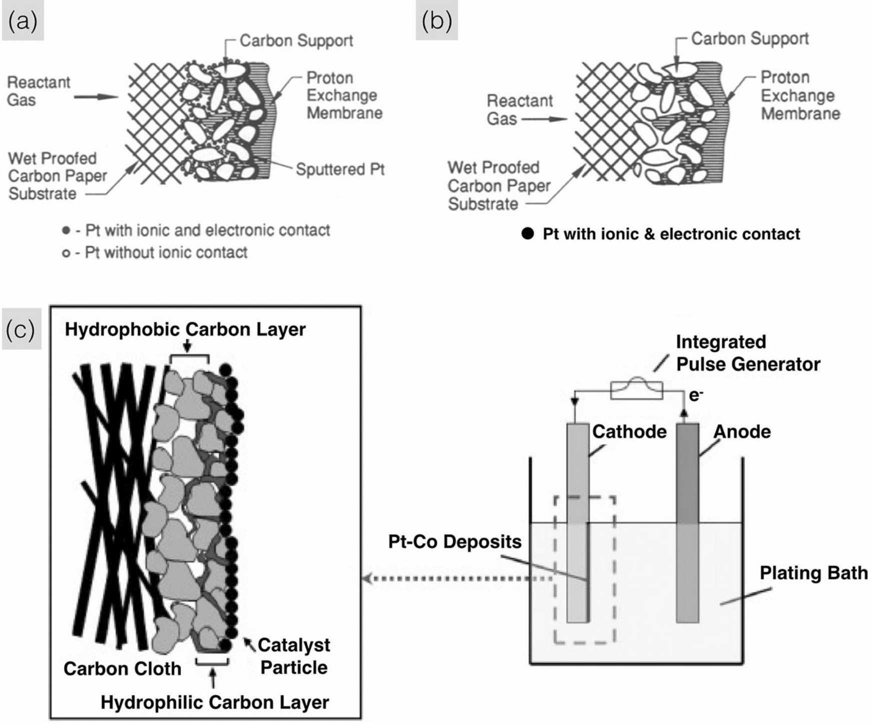

Figure 5. a) Conventional membrane electrode assembly (MEA) composed of Pt/C and a Nafion membrane;[58] b) Catalyst selectively attached to electrically and ionically conductive points;[58] c) Pulsed electrodeposition process for the formation of electrically and ionically connected catalytic sites.[24]

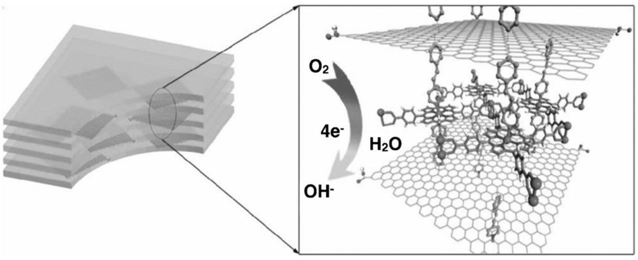

Figure 6. Graphene–MOF hybrid (G-dye-FeP)$_n$, and magnified view of layers inside the framework of (G-dye-FeP)$_n$ showing how graphene sheets intercalated between porphyrin networks.[68]

Recent efforts in the application of MOFs to electrochemical energy storage and conversion include a hybrid of functionalized graphene platelets and MOF for ORR electrocatalysis, which created a uniformly distributed graphene platelet architecture allowing full utilization of the graphene surface (Figure 6).[68] Although graphene has been in the spotlight as a potential electrode material,[69] restacking of graphene layers is one of the practical problems in the fabrication process of electrode with graphene, thus, carbon black or carbon nanotubes (CNTs) were used to prevent the reattachment of graphene layers.[70,71] Although this approach is effective in increasing the utilization of the graphene surface, it is based on the random combination of components while expecting that the statistically most probable configuration would approximate the ideal structure. The bottom-up self-assembly approach, such as the formation of the hybrid of MOF and graphene, provides a way of interconnecting modular nano-architectures, thereby tuning electrode structure by the assembly of parts or building blocks as designed.

4. Analysis of Electrode Architecture

Characterizing what comprises the ideal electrode architecture has not been without challenge because of the overlapping issues arising from the characterization of nanoscale particles and porous materials. The following issues[12] lead to the challenges encountered in such characterization:

i) surface contributions due to large surface-to-volume ratios,
ii) buried interfaces in 3D electrode architectures,
iii) the often amorphous nature of nanostructure solid phases,
iv) interactions of material properties (e.g., electrical and magnetic),
v) analysis of multi-component systems.

Despite these challenges, however, the in-lab suite of material analysis techniques has been used in the characterization of electrode architecture, albeit with differing degrees of success.

4.1. Using TEM to Analyze Nanoscale Morphology and Spatial Distributions of Elements, Crystals, and Chemical States

TEM (transmission electron microscopy) is a very useful tool for the analysis of nanoscale morphology. In addition to providing morphological information, TEM can be combined with ED (electron diffraction), EDS (energy dispersive X-ray spectroscopy), and EELS (electron energy loss spectroscopy) to provide information on crystal structure, chemical composition, and chemical state, respectively; as such, it provides details corresponding to morphological structure. Combining tomography with TEM enables the visualization of the 3D morphology of catalyst/support interfaces. Recently, IL-TEM (identical location TEM) has been developed to track electrocatalyst structural changes before and after electrochemical ORR.[28] This technique can capture the morphological changes that Pt/C undergoes in response to catalyst degradation as a result of agglomeration, detachment, and dissolution of Pt, and carbon corrosion. Furthermore, electrochemical in situ TEM has revealed changes in Li-ion distribution in $LiFePO_4$ structures.[72] These in situ and operando TEM analyses provide a major tool for identifying morphology-related material properties to evaluate electrode architecture stability during electrochemical processes.

4.2. X-ray Imaging and Tomography for Mesoscale Morphology Studies

Although TEM has been a very successful tool for characterizing catalyst, support, and catalyst/support interfaces at the nanoscale, the inherently short inelastic mean free path of electrons makes it difficult to observe material structures on a larger scale ($>0.2\ \mu m$). Increasing the electron voltage and current to enhance the transmission depth can cause electron-beam damage to the material, creating chemical composition artifacts or destroying the structures of the analyzed materials.[73] The morphology of larger scale materials can be observed well using scanning transmission X-ray microscopy (STXM) or ptychography, which also provide information on chemical composition and states. These X-ray-based microscopy and tomography techniques have been used to capture images and create chemical maps of approximately 1 μm $LiFePO_4$ particles during the process of charging and discharging (Figure 7).[74] These imaging techniques offer details into the relationship between particle morphology and Li-ion transport properties, and also provide information on the electrode network architecture by enabling the observation of Li-ion transport.

4.3. Operando Methods for Probing Electrode/Electrolyte Interfaces

The ability to probe chemical changes of different phase materials near electrode interfaces is important for understanding how electrochemical processes destabilize interfaces and for elaborating new architectural design and construction methods to statistically induce more reliable interface con-

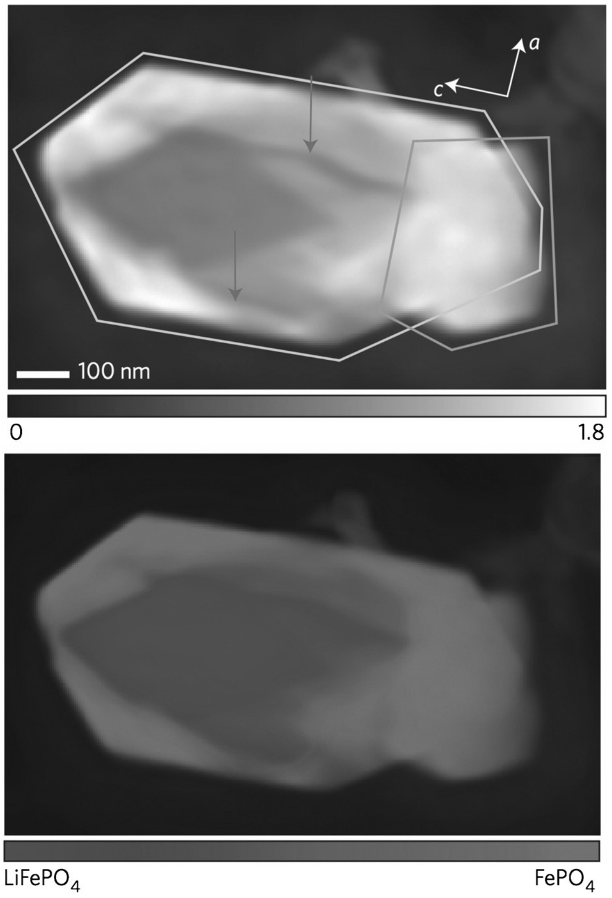

Figure 7. Top: X-ray of a ptychographically reconstructed microscopic image of partially lithiated LiFePO$_4$ at $h\nu = 710$ eV. The scale from 0 to 1.8 is the X-ray absorption by the material at the photon energy of 710 eV. The two gray arrows indicate cracks in the particle. In addition, *a* and *c* crystallographic axes are indicated by white arrow and *b* axis is parallel to X-ray transmission. Bottom: composition map showing the spatial distribution of FePO$_4$ (dark gray) and LiFePO$_4$ (light gray).[74]

nections. Analyzing interfaces is very difficult because the methods to accomplish this must be sensitive enough to detect components in a narrow range but also be able to probe depth to identify different layers.

Of late, synchrotron-based in situ soft X-ray ($h\nu \leq 1$ keV) absorption spectroscopy[75] and ambient pressure X-ray ($h\nu \approx 4$ keV) photoelectron spectroscopy (AP-XPS) have been developed to probe electrified solid/liquid interfaces.[76,77] In situ and operando soft X-ray absorption were used to study the liquid electrolyte species near electrode surfaces. Moreover, the recently developed in situ electrochemical AP-XPS is expected to monitor more sensitively the chemical state of electrode and electrolyte at the "solid electrode/liquid electrolyte" interface under electrochemical potential. Combining these spectroscopic techniques with microscopy will enable the spatial dependence of spectroscopic behavior to be determined, which is crucial in characterizing interface behavior during electrochemical processes.

5. Concluding Remarks

The full potential of electrochemical energy storage and conversion technologies, such as metal–air batteries, water electrolysis, supercapacitors, and fuel cells, is yet to be realized. However, the importance of such technology as the world transitions toward using renewable energy is unquestionable. As such, the design and development of optimized electrode architecture (Figure 8) is the key to large-scale adoption of these technologies. The fundamental goals of an electrode architecture are homogeneous activity distribution, high utilization efficiency, and stability. Establishing a uniform reaction-rate distribution over the completely connected interphase is an important objective in electrode design to minimize over- or under-utilized sites and to provide better stability and performance of the overall system. Two basic archetypes of electrode (interconnected fractal structure and ordered array structure) offer a number of additional sophisticated variations. The architecture combining ordered nanoscale electroactive (electrocatalytic) components and meso- and macroscale hierarchical fractal network structure is crucial for the uniform distribution of reaction rates and stress in the electrode structure by making transfer and conduction properties homogeneous. However, it is still not straightforward to construct a complete interphase network connected to multiple phases by using top-down fabrication technologies. Advanced bottom-up self-assembling synthesis methods, such as electrodeposition and the use of MOFs, might be able to provide a way to create a completely connected interphase network. For stability, electrodes should be designed to have dimensional stability, flexibility to cope with various environments, and no over-

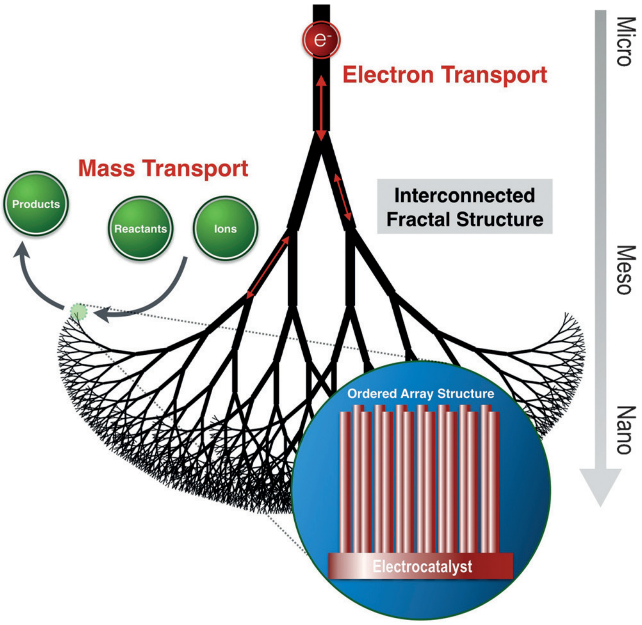

Figure 8. Schematic diagram of the suggested ideal electrode architecture combining the hierarchical fractal structure for mass transport and charge (ion, electron) conduction, and the ordered array structure for electroactive (or electrocatalytic) components.

utilized interfacial active sites. X-ray-based non-destructive structure-probing analysis would allow real-time imaging of the multi-scale 3D structures of electrodes during electrochemical processes. We expect that operando analytical tools for monitoring electrified interfaces could provide information that would facilitate the creation of electrode architectures with homogeneous activity, complete utilization of active sites, and stability.

Acknowledgements

This work was supported by the New & Renewable Energy Core Technology Program of the Korea Institute of Energy Technology Evaluation and Planning (KETEP), granted financial resource from the Ministry of Trade, Industry & Energy, Republic of Korea (20153030031720). J.L. is deeply indebted to the Alexander von Humboldt Foundation fellowship for experienced researchers (1141065).

How to cite: *Angew. Chem. Int. Ed.* **2016**, *55*, 4870–4880
Angew. Chem. **2016**, *128*, 4952–4962

[1] A. J. Bard, L. R. Faulkner, *Electrochemical Methods: Fundamentals and Applications*, Wiley, New York, **2001**.
[2] J. Hagen, *Industrial Catalysis: A Practical Approach*, Wiley, Hoboken, **2006**.
[3] D. R. Rolison, *Science* **2003**, *299*, 1698–1701.
[4] H. R. Kunz, G. A. Gruver, *J. Electrochem. Soc.* **1975**, *122*, 1279–1287.
[5] S.-Y. Huang, P. Ganesan, S. Park, B. N. Popov, *J. Am. Chem. Soc.* **2009**, *131*, 13898–13899.
[6] M. S. Wilson, F. H. Garzon, K. E. Sickafus, S. Gottesfeld, *J. Electrochem. Soc.* **1993**, *140*, 2872–2877.
[7] J. Koresh, A. Soffer, *J. Electrochem. Soc.* **1977**, *124*, 1379–1385.
[8] D. Ma, Z. Cao, A. Hu, *Nano-Micro Lett.* **2014**, *6*, 347–358.
[9] J. Lee, B. Jeong, J. D. Ocon, *Curr. Appl. Phys.* **2013**, *13*, 309–321.
[10] Y. Li, Z.-Y. Fu, B.-L. Su, *Adv. Funct. Mater.* **2012**, *22*, 4634–4667.
[11] J. Baxter, Z. Bian, G. Chen, D. Danielson, M. S. Dresselhaus, A. G. Fedorov, T. S. Fisher, C. W. Jones, E. Maginn, U. Kortshagen, et al., *Energy Environ. Sci.* **2009**, *2*, 559–588.
[12] D. R. Rolison, J. W. Long, J. C. Lytle, A. E. Fischer, C. P. Rhodes, T. M. McEvoy, M. E. Bourg, A. M. Lubers, *Chem. Soc. Rev.* **2008**, *38*, 226–252.
[13] X. Cheng, B. Yi, M. Han, J. Zhang, Y. Qiao, J. Yu, *J. Power Sources* **1999**, *79*, 75–81.
[14] M. H. Eikerling, K. Malek, Q. Wang, in *PEM Fuel Cell Electrocatalysts and Catalyst Layers* (Ed.: J. Zhang), Springer, London, **2008**, pp. 381–446.
[15] A. Amann, W. Gans, *Angew. Chem. Int. Ed. Engl.* **1989**, *28*, 268–276; *Angew. Chem.* **1989**, *101*, 277–285.
[16] G. B. West, J. H. Brown, B. J. Enquist, *Science* **1997**, *276*, 122–126.
[17] J. Lee, J. Kim, T. Hyeon, *Adv. Mater.* **2006**, *18*, 2073–2094.
[18] M. Eikerling, A. A. Kornyshev, E. Lust, *J. Electrochem. Soc.* **2005**, *152*, E24–E33.
[19] M. Uchida, Y.-C. Park, K. Kakinuma, H. Yano, D. A. Tryk, T. Kamino, H. Uchida, M. Watanabe, *Phys. Chem. Chem. Phys.* **2013**, *15*, 11236–11247.
[20] D. E. Stephenson, B. C. Walker, C. B. Skelton, E. P. Gorzkowski, D. J. Rowenhorst, D. R. Wheeler, *J. Electrochem. Soc.* **2011**, *158*, A781–A789.
[21] R. O'Hayre, F. B. Prinz, *J. Electrochem. Soc.* **2004**, *151*, A756–A762.
[22] R. O'Hayre, D. M. Barnett, F. B. Prinz, *J. Electrochem. Soc.* **2005**, *152*, A439–A444.
[23] M. K. Debe, *ECS Trans.* **2012**, *45*, 47–68.
[24] S. Woo, I. Kim, J. K. Lee, S. Bong, J. Lee, H. Kim, *Electrochim. Acta* **2011**, *56*, 3036–3041.
[25] M. K. Debe, *Nature* **2012**, *486*, 43–51.
[26] M. K. Debe, A. K. Schmoeckel, G. D. Vernstrom, R. Atanasoski, *J. Power Sources* **2006**, *161*, 1002–1011.
[27] J. Y. Cheon, T. Kim, Y. Choi, H. Y. Jeong, M. G. Kim, Y. J. Sa, J. Kim, Z. Lee, T.-H. Yang, K. Kwon, et al., *Sci. Rep.* **2013**, *3*, 2715.
[28] J. C. Meier, C. Galeano, I. Katsounaros, A. A. Topalov, A. Kostka, F. Schüth, K. J. J. Mayrhofer, *ACS Catal.* **2012**, *2*, 832–843.
[29] V. Goellner, C. Baldizzone, A. Schuppert, M. T. Sougrati, K. Mayrhofer, F. Jaouen, *Phys. Chem. Chem. Phys.* **2014**, *16*, 18454–18462.
[30] C. K. Chan, H. Peng, G. Liu, K. McIlwrath, X. F. Zhang, R. A. Huggins, Y. Cui, *Nat. Nanotechnol.* **2008**, *3*, 31–35.
[31] A. Magasinski, P. Dixon, B. Hertzberg, A. Kvit, J. Ayala, G. Yushin, *Nat. Mater.* **2010**, *9*, 353–358.
[32] *FY 2014 Merit Review and Peer Evaluation Report*, U.S. Department Of Energy, Washington, DC, **2014**.
[33] A. Kongkanand, M. Dioguardi, C. Ji, E. L. Thompson, *J. Electrochem. Soc.* **2012**, *159*, F405–F411.
[34] J. Lee, *Electro-Oxidation of Small Organic Molecules—Kinetic Instabilities and Spatiotemporal Pattern Formation*, TU Berlin, **2001**.
[35] J. Lee, J. Christoph, P. Strasser, M. Eiswirth, G. Ertl, *J. Chem. Phys.* **2001**, *115*, 1485–1492.
[36] J. Christoph, P. Strasser, M. Eiswirth, G. Ertl, *Science* **1999**, *284*, 291–293.
[37] Y.-J. Li, J. Oslonovitch, N. Mazouz, F. Plenge, K. Krischer, G. Ertl, *Science* **2001**, *291*, 2395–2398.
[38] A. Manthiram, A. V. Murugan, A. Sarkar, T. Muraliganth, *Energy Environ. Sci.* **2008**, *1*, 621–638.
[39] Y. Yue, H. Liang, *J. Power Sources* **2015**, *284*, 435–445.
[40] Y. Nie, L. Li, Z. Wei, *Chem. Soc. Rev.* **2015**, *44*, 2168–2201.
[41] A. Serov, K. Artyushkova, P. Atanassov, *Adv. Energy Mater.* **2014**, *4*, 1301735.
[42] I.-Y. Jeon, C. Kim, G. Kim, J.-B. Baek, *Carbon* **2015**, *93*, 465–472.
[43] L. Gan, M. Heggen, S. Rudi, P. Strasser, *Nano Lett.* **2012**, *12*, 5423–5430.
[44] M. Zhang, Y. Yan, K. Gong, L. Mao, Z. Guo, Y. Chen, *Langmuir* **2004**, *20*, 8781–8785.
[45] K. L. Pickrahn, A. Garg, S. F. Bent, *ACS Catal.* **2015**, *5*, 1609–1616.
[46] *Whisker Technology* (Ed.: A. P. Levitt), Wiley-Interscience, New York, **1970**.
[47] Y. Zhang, N. Wang, S. Gao, R. He, S. Miao, J. Liu, J. Zhu, X. Zhang, *Chem. Mater.* **2002**, *14*, 3564–3568.
[48] R. S. Wagner, W. C. Ellis, *Appl. Phys. Lett.* **1964**, *4*, 89–90.
[49] X. Duan, C. M. Lieber, *Adv. Mater.* **2000**, *12*, 298–302.
[50] X. Duan, C. M. Lieber, *J. Am. Chem. Soc.* **2000**, *122*, 188–189.
[51] A. M. Morales, C. M. Lieber, *Science* **1998**, *279*, 208–211.
[52] M. H. Huang, Y. Wu, H. Feick, N. Tran, E. Weber, P. Yang, *Adv. Mater.* **2001**, *13*, 113–116.
[53] L. Isaacs, D. N. Chin, N. Bowden, Y. Xia, G. M. Whitesides, in *Perspectives in Supramolecular Chemistry* (Ed.: D. N. Reinhoudt), Wiley, New York, **1999**, pp. 1–46.
[54] G. Hornyak, M. Kröll, R. Pugin, T. Sawitowski, G. Schmid, J.-O. Bovin, G. Karsson, H. Hofmeister, S. Hopfe, *Chem. Eur. J.* **1997**, *3*, 1951–1956.
[55] B. A. Korgel, D. Fitzmaurice, *Adv. Mater.* **1998**, *10*, 661–665.
[56] J. W. Long, D. R. Rolison, *Acc. Chem. Res.* **2007**, *40*, 854–862.
[57] S. M. George, *Chem. Rev.* **2010**, *110*, 111–131.

[58] E. J. Taylor, E. B. Anderson, N. R. K. Vilambi, *J. Electrochem. Soc.* **1992**, *139*, L45 – L46.

[59] H. Jeon, J. Joo, Y. Kwon, S. Uhm, J. Lee, *J. Power Sources* **2010**, *195*, 5929 – 5933.

[60] Z.-L. Xiao, C. Y. Han, W.-K. Kwok, H.-H. Wang, U. Welp, J. Wang, G. W. Crabtree, *J. Am. Chem. Soc.* **2004**, *126*, 2316 – 2317.

[61] S. Uhm, H. J. Lee, Y. Kwon, J. Lee, *Angew. Chem. Int. Ed.* **2008**, *47*, 10163 – 10166; *Angew. Chem.* **2008**, *120*, 10317 – 10320.

[62] J. C. Lytle, J. M. Wallace, M. B. Sassin, A. J. Barrow, J. W. Long, J. L. Dysart, C. H. Renninger, M. P. Saunders, N. L. Brandell, D. R. Rolison, *Energy Environ. Sci.* **2011**, *4*, 1913 – 1925.

[63] O. M. Yaghi, H. Li, *J. Am. Chem. Soc.* **1995**, *117*, 10401 – 10402.

[64] Milestone 22: Nature Milestones in Crystallography, can be found under http://www.nature.com/milestones/milecrystal/full/milecrystal22.html, **2014**.

[65] A. Morozan, F. Jaouen, *Energy Environ. Sci.* **2012**, *5*, 9269 – 9290.

[66] G. Férey, F. Millange, M. Morcrette, C. Serre, M.-L. Doublet, J.-M. Grenèche, J.-M. Tarascon, *Angew. Chem. Int. Ed.* **2007**, *46*, 3259 – 3263; *Angew. Chem.* **2007**, *119*, 3323 – 3327.

[67] S. Zhao, H. Yin, L. Du, L. He, K. Zhao, L. Chang, G. Yin, H. Zhao, S. Liu, Z. Tang, *ACS Nano* **2014**, *8*, 12660 – 12668.

[68] M. Jahan, Q. Bao, K. P. Loh, *J. Am. Chem. Soc.* **2012**, *134*, 6707 – 6713.

[69] Y. Sun, Q. Wu, G. Shi, *Energy Environ. Sci.* **2011**, *4*, 1113.

[70] H. Jiang, P. S. Lee, C. Li, *Energy Environ. Sci.* **2013**, *6*, 41 – 53.

[71] S. Woo, J. Lee, S.-K. Park, H. Kim, T. D. Chung, Y. Piao, *J. Power Sources* **2013**, *222*, 261 – 266.

[72] M. E. Holtz, Y. Yu, D. Gunceler, J. Gao, R. Sundararaman, K. A. Schwarz, T. A. Arias, H. D. Abruña, D. A. Muller, *Nano Lett.* **2014**, *14*, 1453 – 1459.

[73] R. F. Egerton, P. Li, M. Malac, *Micron* **2004**, *35*, 399 – 409.

[74] D. A. Shapiro, Y.-S. Yu, T. Tyliszczak, J. Cabana, R. Celestre, W. Chao, K. Kaznatcheev, A. L. D. Kilcoyne, F. Maia, S. Marchesini, et al., *Nat. Photon.* **2014**, *8*, 765 – 769.

[75] J.-J. Velasco-Velez, C. H. Wu, T. A. Pascal, L. F. Wan, J. Guo, D. Prendergast, M. Salmeron, *Science* **2014**, *346*, 831 – 834.

[76] S. Axnanda, E. J. Crumlin, B. Mao, S. Rani, R. Chang, P. G. Karlsson, M. O. M. Edwards, M. Lundqvist, R. Moberg, P. Ross, et al., *Sci. Rep.* **2015**, *5*, 9788.

[77] R. Arrigo, M. Hävecker, M. E. Schuster, C. Ranjan, E. Stotz, A. Knop-Gericke, R. Schlögl, *Angew. Chem. Int. Ed.* **2013**, *52*, 11660 – 11664; *Angew. Chem.* **2013**, *125*, 11874 – 11879.

Received: August 19, 2015
Revised: September 21, 2015